Process-Based Modeling of Infiltration, Soil Loss, and Dissolved Solids on Saline and Sodic Soils

S. K. Nouwakpo, M. A. Weltz, A. Arslan, C. H. Green, O. Z. Al-Hamdan

Abstract. *The Colorado River is a central socio-economic resource of the western U.S. but is vulnerable to excessive salt load. To improve knowledge of the surface processes controlling salt loading, a series of rainfall simulation experiments were conducted in saline rangelands of the upper Colorado River basin (UCRB). In this study, data from these rainfall simulation experiments were used to develop predictive equations for the process-based Rangeland Hydrology and Erosion Model (RHEM). Runoff and soil loss prediction performances were assessed with the Nash-Sutcliffe efficiency (NSE), the coefficient of determination (R^2), and the percent bias (PBIAS). Calibration on 36 individual plots, randomly selected to cover each treatment, yielded improved runoff prediction (NSE = 0.73, R^2 = 0.74, and PBIAS = 6.93%) compared to the non-calibrated RHEM parameter estimation equation (NSE = 0.65, R^2 = 0.68, and PBIAS = 32.03%) when a refined ground cover coefficient was used to estimate the effective hydraulic conductivity (K_e). Soil loss prediction with the calibration data was also improved compared to the non-calibrated parameter estimation equation (NSE = 0.94, R^2 = 0.94, and PBIAS = 4.25% vs. NSE = 0.81, R^2 = 0.85, and PBIAS = 6.47%) when the soil sodium adsorption ratio (SAR) was included in estimation of the sheet and splash erosion parameter (K_{ss}). Improvements in runoff and soil loss predictions with the calibration data were maintained with an independent set of 36 plots from the original rainfall simulation dataset not used for calibration. Overall, soil sodicity was an important consideration in the performance of the newly developed K_{ss} parameterization equation in this study. Performance on sodic soils (SAR $\geq$ 15) gained the most from the inclusion of SAR in the K_{ss} estimation. Salt load was linearly related to soil loss (R^2 = 0.94), and this linear model performed well in estimating runoff salt load from RHEM-predicted soil loss. These new developments will provide a physically based modeling scheme for land managers for predicting rainfall-driven soil and salt load to surface waters of the UCRB.*

Keywords. *Erosion modeling, Hydrology, Rangeland, Salinity prediction, Soil erosion, Water quality.*

The Colorado River is an essential resource in the western U.S. and Mexico, providing municipal water to 40 million people, irrigation water for millions of hectares of land, and other environmental services to wildlife and humans (Bureau of Reclamation, 2005). The salinity of the Colorado River has become a central issue among river and infrastructure managers due to the significant costs (more than $380 million in 2009) of damages caused by salts in the Colorado River (Bureau of Reclamation, 2005). Salinity control efforts have traditionally targeted irrigated lands in the lower Colorado River basin to reduce salt loading to the river system. Nevertheless, the dominant portion (55%) of the total dissolved solids (a measure of salinity) in the Colorado River comes from natural non-irrigated rangelands, mostly in the upper Colorado River basin (UCRB) (Kenney et al., 2009), suggesting further control of the Colorado River's salinity through management actions on these rangelands.

Specific physiographic conditions (saline and sodic parent materials at low basin elevation) in vast expanses of the UCRB create opportunities for high salt loading to the Colorado River (Blackman et al., 1973). These geologic conditions are often exacerbated by low vegetation cover due to low annual precipitation ranging from 150 to 455 mm year^{-1} (NRCS, 2006) and physiologically stringent growth conditions (Cadaret et al., 2016b), leading to accelerated soil erosion. Salts are transported along with soil, and a close association between soil erosion and salt load has been described (Cadaret et al., 2016b; Laronne and Shen, 1982; Ponce et al., 1975) and even used as a predictive tool (Cadaret et al., 2016b; Laronne and Shen, 1982). Laronne and Shen (1982) proposed a basic empirical slope-based model to predict salt load, while Cadaret et al. (2016b) predicted salt load from soil loss information derived from the process-based Rangeland Hydrology and Erosion Model (RHEM).

Submitted for review in November 2017 as manuscript number NRES 12705; approved for publication by the Natural Resources & Environmental Systems Community of ASABE in February 2018.

Mention of company or trade names is for description only and does not imply endorsement by the USDA. The USDA is an equal opportunity provider and employer.

The authors are **Sayjro K. Nouwakpo,** Research Assistant Professor, Department of Natural Resources and Environmental Science, University of Nevada, Reno, Nevada; **Mark A. Weltz,** Research Leader, USDA-ARS Great Basin Rangelands Research Unit, Reno, Nevada; **Awadis Arslan,** Research Scientist, Department of Natural Resources and Environmental Science, University of Nevada, Reno, Nevada; **Colleen H. Green,** Physical Scientist, Bureau of Land Management, National Operations Center, Denver, Colorado; **Osama Z. Al-Hamdan,** Assistant Professor, Department of Civil and Architectural Engineering, Texas A&M University, Kingsville, Texas. **Corresponding author:** Sayjro K. Nouwakpo, University of Nevada, 664 N. Virginia St., Reno, NV 89512; phone: 775-784-6056; e-mail: snouwakpo@cabnr.unr.edu.

The RHEM model was developed from experimental data collected across various rangeland ecological domains of the western U.S. to address the specificity of rangeland systems in the prediction of soil erosion and runoff generation (Nearing et al., 2011). As a process-based model, RHEM was developed as a response to earlier unsatisfactory efforts to apply empirical soil erosion models, such as the Universal Soil Loss Equation (USLE), to rangelands (e.g., Blackburn, 1980; Foster et al., 1981; Hart, 1984; Spaeth et al., 2003). The lumped nature and rigid structure of empirical models make them ill-fitted to address rangeland conditions where biotic and abiotic interactions strongly control surface processes (Weltz et al., 1998). RHEM has been used in many studies to help answer hydrology and erosion questions, including benchmarking results of a jet impingement test for soil erodibility measurement (Lisenbee et al., 2017), evaluating the effect of rangeland conditions and disturbance on hydrologic response (e.g., Al-Hamdan et al., 2015; Belnap et al., 2013; Nouwakpo et al., 2016), proposing new rangeland assessment methods integrating ecohydrologic processes (e.g., M. Hernandez et al., 2013; Weltz et al., 2014; Williams et al., 2016), and evaluating the effect of climate exchange on runoff and erosion (Zhang et al., 2012).

The experimental data used to develop the RHEM model were collected on rangeland sites across the western U.S. with no *a priori* assumption of soil salinity or sodicity effects. Soil salinity and sodium content confer physio-chemical properties that affect soil strength and water content (Agassi et al., 1994; Levy et al., 2003; She et al., 2015; Sumner, 1993; Tang et al., 2006). With the exception of sodium ions, an increase in soil water electrolytes is associated with the development of strong water-stable soil aggregates, which in turn (1) are less susceptible to slaking and detachment by erosion and (2) facilitate infiltration, further reducing the ability of runoff water to detach and transport sediments (Agassi et al., 1994; Levy et al., 2003). However, an increase in sodium content has a detrimental effect on aggregate strength through expansion and dispersion of soil clay particles, often leading to an increase in aggregate slaking, surface sealing, and increased runoff and erosion volumes (Levy et al., 2003; Sumner, 1993; Tang et al., 2006).

Saline and sodic sites are not currently addressed by the RHEM model due to a lack of equations that specifically target these rangeland sites. In the original experimental data used in the development of RHEM, a saltbrush site near Meeker, Colorado, with soils of sodic parent material was found to be an outlier in the amount of erosion generated at the site compared to other study sites (Simanton et al., 1991). As an outlier, this site was later excluded in the development of RHEM (Nearing et al., 2011). Recent efforts to develop a process-based modeling framework to predict runoff, soil erosion, and salt load from saline rangelands of the UCRB has produced parameter estimation equations specific to saline conditions (Cadaret et al., 2016a). Using experimental data collected at two saline sites in the UCRB, Cadaret et al. (2016a) proposed scaled versions of the traditional RHEM equations for effective soil hydraulic conductivity (K_e) and the sheet and splash erosion parameter (K_{ss}). The work of Cadaret et al. (2016a) highlights observed differences in the hydrologic response of saline soils compared to the non-saline and non-sodic soils represented in traditional RHEM equations but was of limited physiographic scope.

The objective of this study was to (1) develop new parameter estimation equations for K_e and K_{ss} from experimental data collected across a broader physiographic scope than achieved by Cadaret et al. (2016a) and incorporate salinity and sodicity dependent soil properties in these equations and (2) test the performance of these newly developed equations to predict runoff, soil loss, and salt load.

Methodology

Experimental Data Description

The data used in this study were collected as part of a broader effort to improve knowledge of water, sediment, and salt transport in the UCRB. A series of rainfall simulation experiments were conducted at sites in the UCRB that have been identified as high salt contributors to the river system. Data from rainfall simulation experiments at six salt-affected desert rangeland sites were used in this study (fig. 1). These data were collected during plot-scale rainfall simulation experiments conducted between 2014 and 2016. Plots measured 6 m × 2 m and were selected to be collectively representative of the site being evaluated. At five of the six sites, intensities corresponding to 2, 10, 25, and 50-year storm return intervals were applied and replicated three times using one plot per replicate. At the sixth site, the research question pursued was to understand the link between vegetation cover and soil and salt transport on a gradient of vegetation cover. At this site, a unique 25-year return period rainfall intensity was used on four replicates of three vegetation cover categories, yielding a total of 12 plots. Overall, with 12 plots per site, a total of 72 rainfall simulations were run and used in this study.

Rainfall simulations were performed with the Walnut Gulch Rainfall Simulator set at a nozzle pressure of 55 kPa and a height of 2.44 m (Paige et al., 2004). During each rainfall simulation experiment, runoff was conveyed in a supercritical flume in which runoff stage was monitored with a flowmeter (Teledyne 4230, Isco, Inc., Lincoln, Neb.) and converted into runoff discharge using a calibrated stage-discharge equation. Runoff discharge measurements made with the Teledyne 4230 flowmeter were available every 15 s and supplemented with manual measurements every 5 to 6 min throughout a rainfall simulation. These manual measurements consisted of measuring the amount of time needed to fill a 3.8 L bucket and were used as verification of the automatically measured runoff discharge.

Runoff samples were collected in 1 L bottles every 3 min throughout each rainfall simulation and were used to determine sediment concentration by oven-drying at 105°C and weighing the amount of sediment contained in the sampled volume. These runoff and sediment data provided the instantaneous runoff discharge (q_t) and sediment discharge rate (qs_t) at timed intervals used to determine the cumulative runoff (SR) and total soil loss (SL) produced by each event.

In addition, runoff water quality samples were collected in 50 mL vials every 1.5 min and analyzed in the laboratory

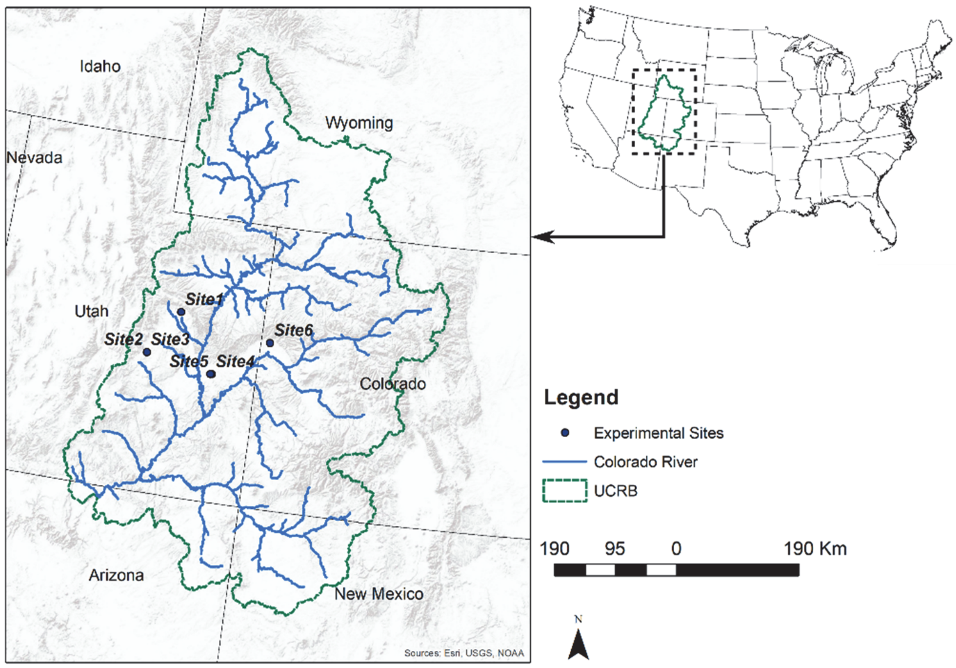

Figure 1. Map of the upper Colorado River basin (UCRB) in the U.S., showing the location of the six sites where rainfall simulation experiments were conducted to produce the data used in this study.

for the concentrations of various ions. Water quality samples were immediately refrigerated in the field and kept at 0°C until analysis in the laboratory. Measured ions were Cl^-, SO_4^{2-}, NO_3^-, Ca^{2+}, Mg^{2+}, Na^+, K^+, and NH_4^+. Cations Ca^{2+} and Mg^{2+} were quantified using atomic absorption spectroscopy, while K^+ and Na^+ concentrations were measured by atomic emission spectroscopy using an atomic absorption (AA) spectrometer (PerkinElmer, Waltham, Mass.). A Lachat Quickchem Flow Injection Analysis+ instrument (Hach Co., Loveland, Colo.) was used to determine ammonium (NH_4^+) concentration. Anions (NO^{2-}, NO^{3-}, SO_4^{2-}, and Cl^-) in runoff water were measured using an ion chromatograph (IC) (Dionex Co., Sunnyvale, Cal.) with an AS18-4µ column. The total dissolved solids (TDS) is often used to measure water salinity. In this study, cumulative TDS was estimated as the sum (in mg L^{-1}) of Cl^-, SO_4^{2-}, NO_3^-, Ca^{2+}, Mg^{2+}, Na^+, K^+, and NH_4^+ lost with the runoff water.

Soil cores were collected at each site to determine specific soil physio-chemical properties before and after rainfall simulation. Pre-rainfall soil cores were taken outside of the rainfall simulation plots at random locations on a hillslope to be representative of initial conditions for multiple plots. Soil cores were collected using a 25 cm long AMS split core sampler with a 5 cm inside diameter at three locations under the vegetation canopy and at three bare soil (interspace) locations. At each soil sample location, the soil cores were split into a surface sample and two subsurface samples (0 to 1 cm, 1 to 5 cm, and 5 to 10 cm). Samples corresponding to each microsite (vegetation vs. interspace) were mixed to make one composite soil sample for each microsite. The soil samples were stored in plastic bags and refrigerated along with the water quality samples at 0°C. Soil chemistry was evaluated by measuring soluble-phase cations and anions in soil solution extracted by immiscible displacement (Mubarak and Olsen, 1976). As with the runoff water quality, soil soluble-phase cations were measured with the AA spectrometer, while soluble-phase anions (NO^{2-}, NO^{3-}, SO_4^{2-}, and Cl^-) were measured with the Dionex IC with an AS11-HC column. Soil mineral N (NO^{2-}, NO^{3-}, and NH_4^+) was extracted using 1.5 M KCl (Bundy and Meisinger, 1994) and quantified on the Lachat system. Measurements of pH and electrical conductivity (EC) were performed on the soil solutions obtained by immiscible displacement. In this study, the sodium adsorption ratio (SAR) of the soil surface layer after rainfall was used to characterize the prevalence of sodium in the soil and was calculated with the following equation:

$$\mathrm{SAR} = \frac{\mathrm{Na}^+}{\sqrt{\tfrac{1}{2}\left(\mathrm{Ca}^2 + \mathrm{Mg}^{2+}\right)}} \tag{1}$$

where Na^+, Ca^{2+}, and Mg^{2+} are the concentrations of these respective ions (mmol$_c$ L^{-1}).

RHEM Model

RHEM is a process-based model developed by the USDA-ARS to predict runoff and sediment yield on rangelands. The first generation of this model, RHEM v1.0 (Nearing et al., 2011), was derived from the same scientific foundation as the Water Erosion Prediction Project (WEPP; Flanagan and Nearing, 1995) but with cropland-specific equations replaced with new parameter estimation functions specifically developed from rangeland data. Data from a total of 204 experimental plots at 49 rangeland sites distributed across 15 states of the western U.S. were used in this first iteration of RHEM (Nearing et al., 2011). RHEM v1.0 used vegetation characteristics, soil properties, and topography to estimate hydraulic and hydrologic parameters, which were combined with climate or hydrologic input to drive a kinematic wave model and solve for the sediment continuity equation. As in the WEPP model, RHEM v1.0 used the excess shear-stress concept to model concentrated flow erosion. Subsequent improvements and adjustments to the model have resulted in the second generation of RHEM (v2.0 and currently v2.3, used in this study), which substituted the shear-stress concept with the stream power model for concentrated flow erosion prediction (Al-Hamdan et al., 2015). Major new scientific developments incorporated in RHEM v2.0 and higher versions include (Hernandez et al., 2017): new equations to capture the effect of rangeland disturbance on soil erosion and infiltration processes, a dynamic solution to the continuity equation to address the often observed decrease in soil erodibility with time after a disturbance, and a framework to evaluate the runoff and erosion risks and benefits associated with disturbances such as fire, climate change, and rangeland management practices. RHEM is available as a freely available web interface that takes the following primary inputs: vegetation canopy cover by lifeform (i.e., annual grasses and forbs, shrubs, and sod grasses), and soil texture (based on the USDA classification) and slope to estimate hydraulic and hydrologic parameters, namely, effective hydraulic conductivity (K_e) and sheet and splash erodibility (K_{ss}). These hydraulic parameters are then combined with climate information to run long-term hydrologic simulations and produce expected annual sediment yields and runoff volumes. Alternatively, RHEM can be executed off-line on a single rainfall event with a standalone desktop executable that applies the kinematic wave and sediment continuity equations to a parameter file containing hydraulic and hydrologic parameters (including K_e and K_{ss}) estimated using appropriate RHEM parameter estimation equations. In this single-event simulation approach, hydrologic input is provided as a time series of instantaneous rainfall intensities (mm h^{-1}) in conjunction with hydraulic and hydrologic parameters to predict runoff discharge and sediment yield at the same temporal resolution. This single-event version of RHEM v2.3 was used in this study because it was suitable for (1) evaluating RHEM on rainfall simulation data and (2) applying optimization routines to develop new parameter estimation equations.

RHEM Calibration

Six plots were selected at each experimental site, for a total of 36 plots, to calibrate RHEM for saline sites, ensuring that each intensity simulated at the site was represented at least once in the calibration dataset. The calibration was performed in two steps to determine the best parameter sets for (1) runoff prediction and (2) soil loss prediction. The numerical optimization was performed using a Markov Chain Monte Carlo (MCMC) method (NRCS, 2006) implemented in SPOTPY (Houska et al., 2015), a model optimization tool written in the Python programming language.

To optimize runoff prediction, the RHEM parameters adjusted for each plot were the soil saturation ratio (SAT), the effective hydraulic conductivity (K_e, mm h^{-1}), the mean capillary drive (G, mm), the variable (ALF) in the Smith-Parlange infiltration equation, and the coefficient of variability (CV) of the hydraulic conductivity. These parameters were estimated in a multi-objective optimization scheme in which errors in both total runoff (SR, L) and 1 min increment instantaneous discharges (q_t, mm h^{-1}) were minimized throughout the rainfall event. The instantaneous discharges used as observations were interpolated from observed discharges that may not systematically occur at exactly 1 min time increments and were compared to predicted discharges at the same time increments. This multi-objective optimization procedure allowed the estimation of parameters that adequately predicted SR while matching as closely as possible the detailed hydrograph of a rainfall event.

For erosion prediction, the sheet and splash erodibility (K_{ss}) was estimated using a separate multi-objective parameter optimization in which errors in total soil loss (SL, kg) and 1 min increment instantaneous sediment discharge rates (qs_t, g s^{-1}) were minimized. For both runoff and soil erosion parameter estimations, the final selection of parameters was done for each calibration plot by choosing the set of parameters that simultaneously minimized the error in cumulative runoff and total soil loss (SR and SL) and belonged to the 5% best performers in matching the detailed hydrograph and sedograph. A total of 36 parameter sets were produced, corresponding to the 36 calibration events.

Parameter Estimation Equations and Salt Load Prediction on Saline Sites

Parameter estimations equations have been developed for RHEM to translate soil biophysical characteristics into hydrology and hydraulics parameters. Currently, equations exist to estimate K_e, K_{ss}, and the Darcy-Weisbach friction factor (F) from equations using ground and vegetation cover information as well as soil texture. For K_e and K_{ss}, the current RHEM equations are:

$$K_e = a\exp\left(b\left(\text{basal} + \text{litter}\right)\right) \tag{2}$$

$$K_{ss} = 10^{\left(c + d\cdot\text{ground cover} + f\cdot\text{foliar cover} + g\cdot\text{slope}\right)} \tag{3}$$

where coefficients a and b differ as a function of soil texture and vegetation community type (i.e., shrub, sod grass, bunch grass and forbs, and annual grass), while coefficients c, d, f, and g are functions of vegetation community type and ground cover. Basal, litter, ground cover, and foliar cover are expressed in areal fractions. Basal cover represents the proportion of the soil surface that is in contact with the bases of plants. Litter cover is the proportion of the soil surface protected by detached vegetation residues. Ground cover is the sum of basal, litter, rock, and cryptogam cover. Foliar cover is the fraction of the land surface that is occupied by the projection of plant leaves onto the soil surface.

Parameters a, b, c, d, f, and g were developed from a large dataset (more than 200 plots) of rainfall simulation experiments across the western U.S. and represent a wide range of rangeland ecosystem types and conditions.

In this study, the K_e and K_{ss} values optimized using the MCMC routine (K_eOpt and K_{ss}Opt) were compared to the values (K_eRHEM, K_{ss}RHEM) predicted by the current version of RHEM for the calibration plots. The differences (ΔK_e and ΔK_{ss}) and ratios (rK_e and rK_{ss}) between the optimized and RHEM-predicted values were calculated and related to soil biophysical characteristics and salinity. Linear regressions were performed between ΔK_e, ΔK_{ss}, rK_e, and rK_{ss}, and canopy cover, fraction of bare ground, sodium adsorption ratio (SAR), electrical conductivity (EC), silt content, and slope. With a total of 36 calibration data points for this analysis, each explained variable was regressed against one explanatory variable at a time to prevent over-parameterization and maintain adequate statistical power.

From the linear regressions linking soil and vegetation attributes to K_e and K_{ss} differences and ratios, factors accounting for the gap between the RHEM-predicted and optimized K_e and K_{ss} values were identified by selecting those exhibiting statistically significant effects on ΔK_e, rK_e, ΔK_{ss}, and rK_{ss}. Factors with statistically significant effects were then evaluated against current terms used in the RHEM parameter estimation equations (eqs. 2 and 3). Factors with statistically significant effects that were already present in equations 2 and 3 suggest a modification of the coefficients applied to those terms in the equations. Factors not previously accounted for in equations 2 and 3 are introduced as new terms according to the nature of their relationships with the RHEM-predicted parameters. For the statistical significance of a factor in the parameter differences (ΔK_e and ΔK_{ss}), the new parameter (K_n) is calculated as:

$$K_n = K_n\text{RHEM} + \left(AX + B\right) \tag{4}$$

where X is one of the six factors (canopy cover, bare ground, SAR, EC, silt content, and slope), and A and B are significant coefficients of the linear regression where these factors have a significant effect.

Likewise, when the ratios (rK_e and rK_{ss}) exhibit a significant effect of a given parameter, K_n is defined as:

$$K_n = K_n\text{RHEM}\left(AX + B\right) \tag{5}$$

When more than one factor was found to have a statistically significant effect on a parameter K_n, the final correction equation retained was developed sequentially by first incorporating the factor with the highest R^2, recomputing the ΔK_n or rK_n values, and relating these values to the subsequent factors to verify that any statistically significant effect remained. For example, if bare ground had a statistically significant effect on ΔK_e and EC had a significant effect on rK_e with $R^2_{\text{bare}} > R^2_{\text{EC}}$, then K_e would be corrected for bare ground first [$K_{e\text{bare}} = K_e\text{RHEM} + (A \times \text{bare} + B)$], r$K_e$ would be recalculated as $K_e\text{Opt} / K_{e\text{bare}}$, and this new variable would be re-evaluated against EC to see if the initial statistical significance remained.

A predictive linear model was built with the calibration data between SL and TDS and tested on the validation data.

Evaluation of Parameter Estimation Equations and Salt Load Prediction

The performance of the adjusted parameter estimation equations (eqs. 4 and 5) was assessed by comparing erosion and runoff predictions with the amended parameters K_n to those obtained with equations 2 and 3. Model performance metrics used for this comparison are the coefficient of determination (R^2), Nash-Sutcliffe efficiency (NSE), and percent bias (PBIAS):

$$R^2 = 1 - \frac{\sum_{i=1}^{n}\left(Y_{lm,i} - Y_{o,i}\right)^2}{\sum_{i=1}^{n}\left(Y_{o,i} - \overline{Y_o}\right)^2} \tag{6}$$

$$\text{NSE} = 1 - \frac{\sum_{i=1}^{n}\left(Y_{p,i} - Y_{o,i}\right)^2}{\sum_{i=1}^{n}\left(Y_{o,i} - \overline{Y_o}\right)^2} \tag{7}$$

$$\text{PBIAS} = \left[\frac{\sum_{i=1}^{n}\left(Y_{p,i} - Y_{o,i}\right)\times 100}{\sum_{i=1}^{n} Y_{o,i}}\right] \tag{8}$$

where Y_o, Y_p, and Y_{lm} are respectively the observed, RHEM-predicted, and linear model prediction between Y_o and Y_p for runoff or soil loss, while $\overline{Y_o}$ is the average of all observations.

These performance metrics were calculated for the 36 calibration data points and the 36 validation data points. The linear model for salt load prediction was also evaluated with these performance metrics. Figure 2 shows a flowchart of the experimental data, describes its content, and illustrates how it was used to develop and test the new parameter estimation equations. Additionally, Welch's t-test was used to compare the validation and calibration data to ensure equal means of input parameters between these two populations. Statistical analyses were conducted in R (R Development Core Team, 2015), and a probability of 0.05 was used as threshold of statistical significance.

Sensitivity Analysis of New K_e and K_{ss} Equations

A sensitivity analysis was performed on the newly developed K_e and K_{ss} equations using a Monte Carlo method (Hernandez et al., 2017). This analysis consisted of perturbing the new coefficients that were introduced into equations 2 and 3 to improve the K_e and K_{ss} predictions for saline soils and then evaluating the effect of these perturbations on runoff and soil loss predictions. For a given coefficient, in either the K_e or K_{ss} equation, a total of 2,000 Monte Carlo simulations were performed during which the value of the coefficient was randomly changed between its average value (α) and $\pm 0.5\alpha$, with an increment of $\alpha/200$. At each Monte Carlo iteration, the runoff or soil loss data (depending on whether K_e or K_{ss} was evaluated) were saved and compared to the predicted runoff or soil loss data when α was used in the corresponding parameter estimation equation.

Results

Calibration of RHEM K_e and K_{ss} for Saline Sites

Figure 3 shows that the distributions of slope, canopy cover, bare ground, rainfall intensity, EC, and SAR were

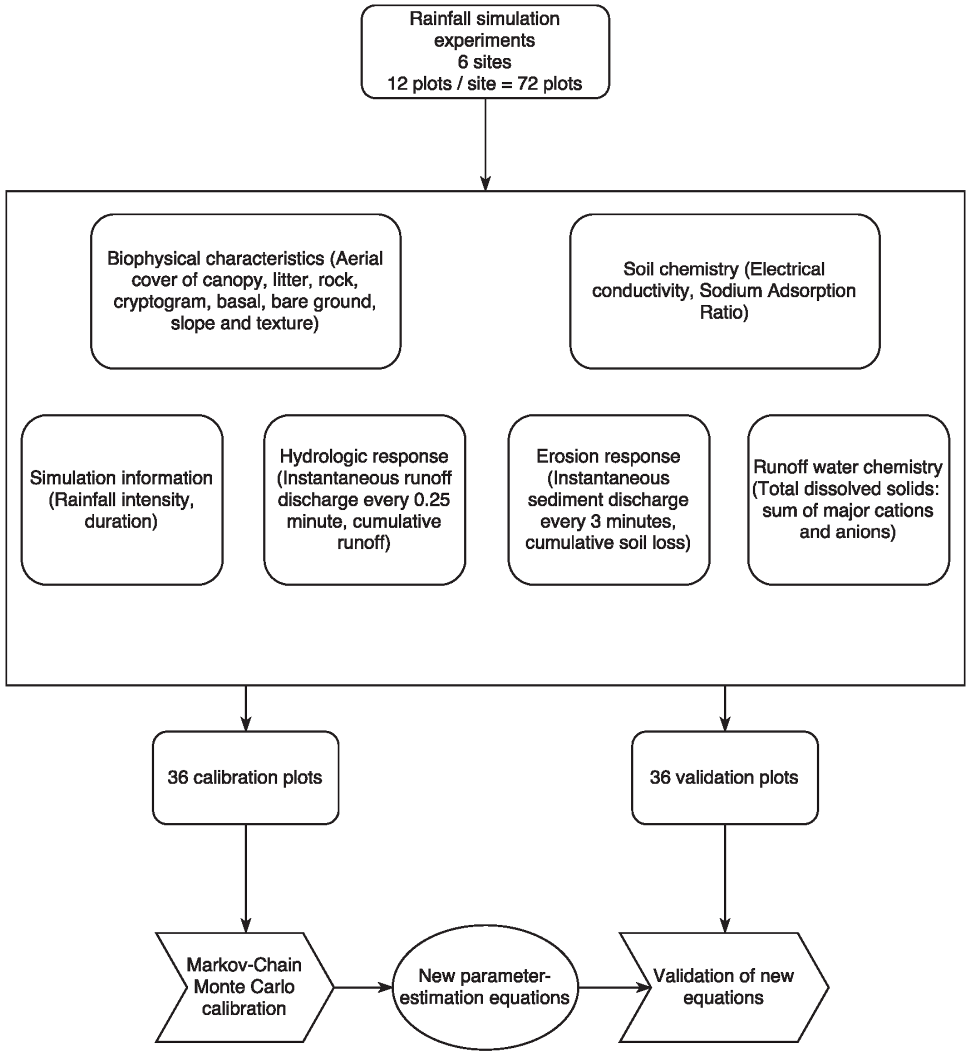

Figure 2. Flowchart of experimental data used for development and validation of new parameter estimation equations on saline sites.

similar across the calibration and validation data. Welch's t-test on each of these input parameters revealed p-values systematically greater than 0.05, suggesting that mean parameter values were statistically identical across the calibration and validation data. Figures 4 and 5 show the results of the runoff and soil loss prediction on the 36 calibration data points using equations 2 and 3 to estimate K_e and K_{ss}. The NSE and R^2 values for runoff were 0.56 and 0.68, respectively, suggesting that the relationships between soil biophysical properties and K_e represented in equation 2 were roughly consistent with the observed patterns in runoff and infiltration at the experimental sites. Equation 2 underpredicted K_e, resulting in a positive bias in predicted cumulative runoff depths (predicted runoff > observed runoff, PBIAS = 32.03%). Soil loss was predicted with an NSE of 0.81 and R^2 of 0.85, with a negative bias (PBIAS = -6.47%). This negative bias in soil loss prediction contrasts with the positive bias in runoff noted in figure 4, which indicates an underprediction of soil erodibility.

The differences and ratios between numerically optimized and RHEM-estimated K_e and K_{ss} (with eqs. 2 and 3) are related to the soil and vegetation factors in table 1. Bare ground fraction was the main soil factor that displayed a statistically significant relationship with ΔK_e values ($p = 0.01$). As bare ground increased, the difference between optimized and RHEM-predicted K_e (eq. 2) values decreased. The ratio (rK_e) of optimized to RHEM-predicted K_e exhibited statistically significant and positive correlations with canopy cover and electrical conductivity ($p = 0.015$ and 0.027, respectively). The performance of K_e values corrected for these statistically significant parameters on the calibration data are shown in table 2. For the calibration data, bare-ground-adjusted K_e values using equation 4 improved |PBIAS| (|-7.89%| < |32.02%|) and NSE (0.64 > 0.56) while maintaining predictive power (R^2 = 0.68) compared to the performance obtained with equation 2. Correcting K_e for the effect of EC on rK_e with equation 5 also yielded improved performance (NSE = 0.74, R^2 = 0.76, and PBIAS = -6.13%) compared to equation 2. The correction of K_e for the effect of canopy cover improved NSE (0.67) and R^2 (0.76) but did not substantially affect PBIAS (27.27%).

The current K_e estimation equation in RHEM (eq. 2) is a function of the sum of basal cover and litter cover and thus an inverse function of bare ground. Our finding of a significant relationship between ΔK_e and bare ground suggests that coefficient b in equation 2 did not adequately predict hydrau-

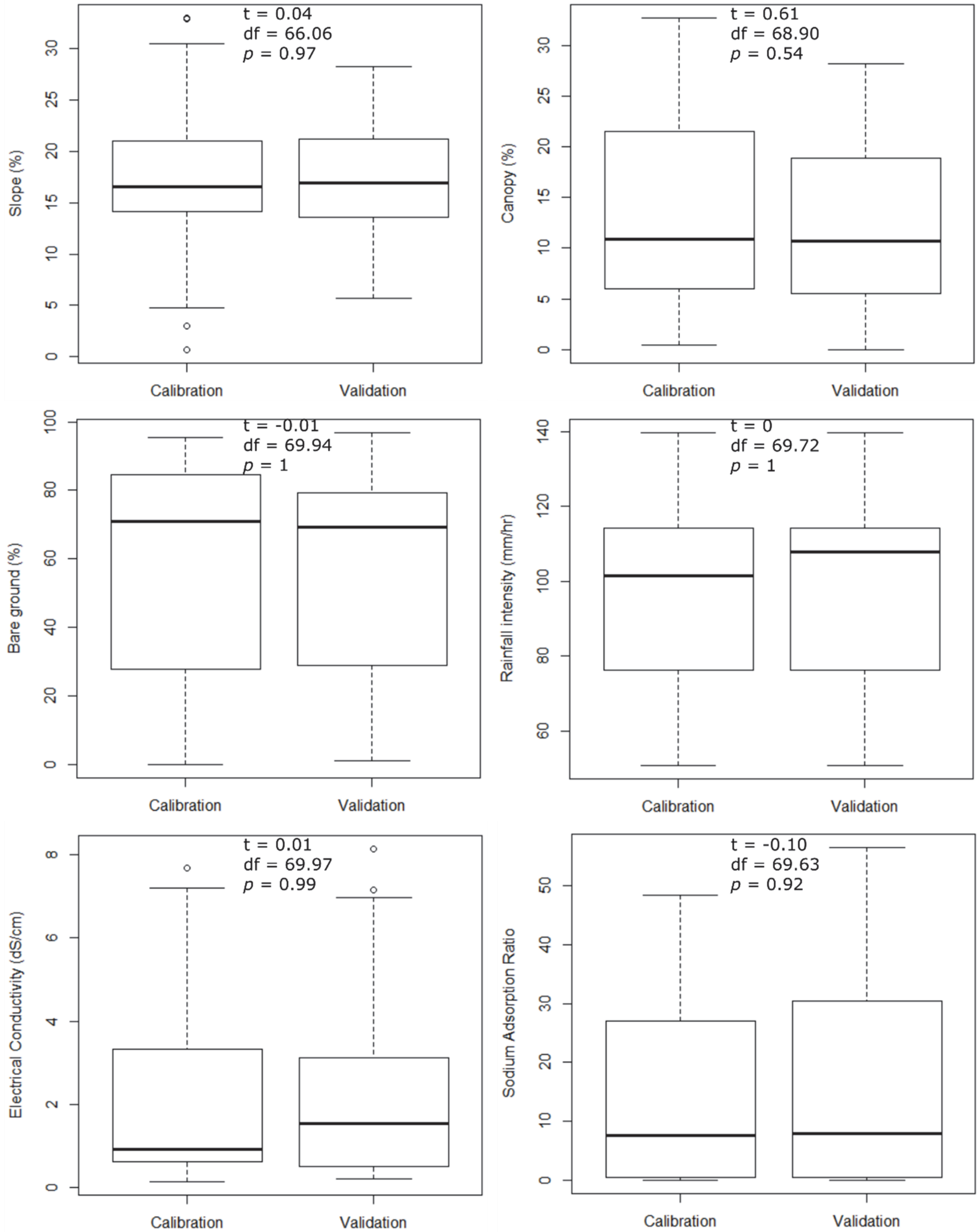

Figure 3. Distribution of slope, canopy cover, bare ground, and rainfall intensity across plots used for calibration and validation data showing the results of Welch t-test means comparison (t = Welch t statistic, df = degree of freedom, and *p* = p-value). Statistically significant differences are defined at p < 0.05.

lic conductivity on the saline sites in this study and thus required further adjustments. An MCMC optimization procedure was performed on coefficient b, which yielded a new coefficient: $b' = 1.55b$. Correcting K_eRHEM values for the effect of bare ground using b' instead of b nullified the statistical effect of canopy cover and EC on the newly computed rK_e ($R^2 = 0.01$ and p = 0.637 for canopy cover, and $R^2 = 0.10$ and p = 0.068 for EC). Canopy cover and EC were then dropped from the analysis as potential factors influencing K_e. The new equation for K_e is then:

$$K_e = a\exp\left(1.554b\left(\text{basal} + \text{litter}\right)\right) \tag{9}$$

The performance of equation 9 on the calibration data was overall better than that of the additive correction model for bare ground (table 2), with NSE = 0.73, PBIAS = 6.93%, and $R^2 = 0.74$.

Differences and ratios between the optimized and RHEM-predicted K_{ss} values show significant effects only for SAR (table 1). The values of ΔK_{ss} and SAR are related through a positive relationship ($R^2 = 0.26$, p = 0.002), while

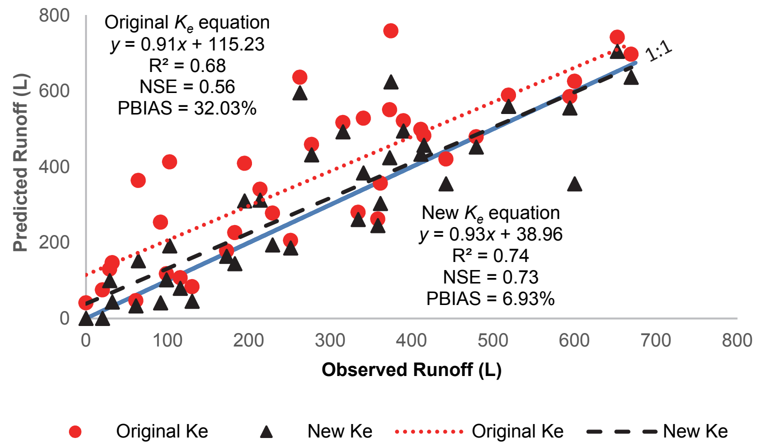

Figure 4. Observed versus predicted runoff for 36 rainfall simulation calibration plots using the current and the newly developed estimation equations for hydraulic conductivity (K_e).

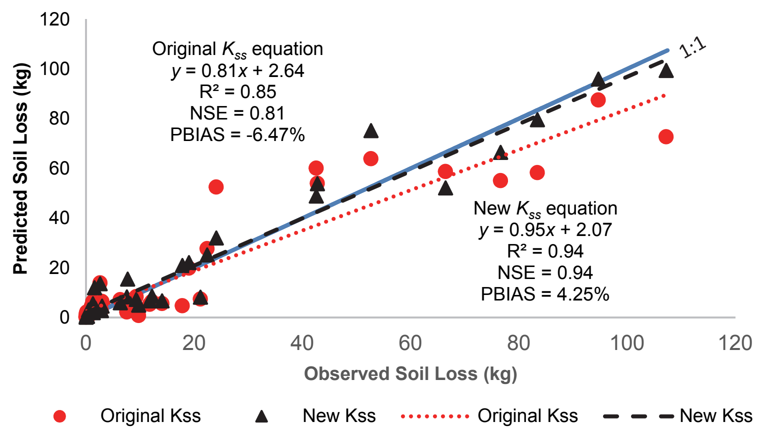

Figure 5. Observed versus predicted soil loss for 36 rainfall simulation calibration plots using the current and the newly developed estimation equations for sheet and splash erodibility (K_{ss}).

Table 1. Linear regressions of explanatory variables (canopy, bare ground, sodium adsorption ratio, silt content, and slope) against differences and ratios between numerically optimized and predicted effective hydraulic conductivity (K_eOpt and K_eRHEM, respectively) and sheet and splash erodibility (K_{ss}Opt and K_{ss}RHEM, respectively). Predicted K_eRHEM and K_{ss}RHEM were calculated from parameter estimation equations of the Rangeland Hydrology and Erosion Model (RHEM v2.3). Coefficients in bold are statistically different from zero at 95% confidence level.

X	K_eOpt – K_eRHEM	K_eOpt / K_eRHEM	K_{ss}Opt – K_{ss}RHEM	K_{ss}Opt / K_{ss}RHEM
Canopy	0.315X + 1.818	**0.097**X + 1.166	309.571X + 1628.354	-0.010X + **1.358**
	R^2 = 0.11, p = 0.057	R^2 = 0.18, p = 0.015	R^2 = 0.02, p = 0.429	R^2 = 0.01, p = 0.585
Bare ground	**-0.117**X + **13.058**	0.004X + **2.204**	45.870X + 3303.325	0.000X + **1.240**
	R^2 = 0.19, p = 0.010	R^2 = 0.00, p = 0.747	R^2 = 0.01, p = 0.679	R^2 = 0.00, p = 0.943
Sodium adsorption ratio	-0.114X + **7.883**	0.028X + **1.967**	**642.452**X – 4672.942	**0.021**X + **0.876**
	R^2 = 0.05, p = 0.233	R^2 = 0.05, p = 0.231	R^2 = 0.26, p = 0.002	R^2 = 0.13, p = 0.042
Electrical conductivity	-0.245X + **6.692**	**0.365**X + **1.624**	2722.687X – 392.805	0.001X + **1.214**
	R^2 = 0.00, p = 0.716	R^2 = 0.15, p = 0.027	R^2 = 0.10, p = 0.071	R^2 = 0.00, p = 0.992
Silt content	-0.084X + **10.437**	0.026X + 1.143	37.804X + 3981.435	-0.012X + **1.827**
	R^2 = 0.04, p = 0.282	R^2 = 0.06, p = 0.167	R^2 = 0.00, p = 0.835	R^2 = 0.06, p = 0.172
Slope	0.207X + 2.480	0.026X + **1.950**	447.590X – 2273.502	0.021X + **0.840**
	R^2 = 0.04, p = 0.256	R^2 = 0.01, p = 0.592	R^2 = 0.03, p = 0.325	R^2 = 0.04, p = 0.296

rK_{ss} relates to SAR with much less predictability (R^2 = 0.13, p = 0.042). Correcting RHEM K_{ss} values for SAR with both the additive (eq. 4) and multiplicative (eq. 5) models resulted in an improvement of NSE (0.94 and 0.89 vs. 0.81) and R^2 (0.94 and 0.93 vs. 0.85) for soil loss prediction compared to the current RHEM K_{ss} estimation equation (table 2). While the bias achieved with the additive model (PBIAS = 4.25%) matched that achieved with equation 3, a greater bias was noted when the multiplicative model was used for K_{ss} correction (PBIAS = 17.18%). The additive model was then retained to adjust K_{ss} for SAR.

Table 2. Nash-Sutcliffe efficiency (NSE), percent bias (PBIAS), and coefficient of determination (R^2) of RHEM prediction with parameter estimation equations for hydraulic conductivity (K_e) and sheet and splash erodibility (K_{ss}) corrected for bare ground percentage (Bare), electrical conductivity (EC), and sodium adsorption ratio (SAR) through linear functions *f*.

		Calibration			Validation		
		NSE	PBIAS (%)	R^2	NSE	PBIAS (%)	R^2
Runoff	$K_e = K_e\text{RHEM} + f(\text{Bare})$	0.64	-7.89	0.68	0.85	-16.03	0.88
	$K_e = K_e\text{RHEM}' = G(\text{Bare})$[a]	0.73	6.93	0.74	0.88	5.41	0.89
	$K_e = K_e\text{RHEM} \times f(\text{EC})$	0.74	-6.13	0.76	0.84	-17.15	0.88
	$K_e = K_e\text{RHEM} \times f(\text{Canopy})$	0.67	27.27	0.76	0.75	15.86	0.77
Soil loss	$K_{ss} = K_{ss}\text{RHEM} + f(\text{SAR})$	0.94	4.25	0.94	0.69	-3.82	0.73
	$K_{ss} = K_{ss}\text{RHEM} \times f(\text{SAR})$	0.89	17.18	0.93	0.83	6.04	0.83

[a] K_eRHEM′ is an update of K_eRHEM as a non-linear function *G* of bare ground with re-estimated bare ground coefficient using Markov Chain Monte Carlo parameter estimation.

Validation of the New K_e and K_{ss} Equations for Saline Sites

Table 2 and figures 6 and 7 show the results of the runoff and soil loss prediction with the new K_e and K_{ss} equations on the 36 validation plots. The K_e values estimated with equation 9 predicted runoff on the 36 validation plots with slightly improved NSE (0.88) and R^2 (0.89) over the original RHEM equation (eq. 2) (NSE = 0.83 and R^2 = 0.85). The runoff prediction bias was substantially improved for these validation plots, dropping from PBIAS = 12.05% with equation 2 to PBIAS = 5.41% when the newly developed equation 9 was used.

The sheet and splash erodibility (K_{ss}) was reasonably predicted on the validation data when SAR was added to the K_{ss} prediction. Compared to the original K_{ss} equation, the use of the SAR-adjusted K_{ss} equation improved soil loss prediction from NSE = 0.38, R^2 = 0.6, and PBIAS = -24.25 to NSE = 0.69, R^2 = 0.73, and PBIAS = -3.82% (fig. 7). Nevertheless, the validation NSE (0.69) and R^2 (0.73) declined compared to the calibration performance (NSE = 0.94 and R^2 = 0.94) due to increased error propagation from runoff prediction to soil loss estimates in the validation data. In effect, calibrated K_e values were used in the estimation of soil loss for evalu-

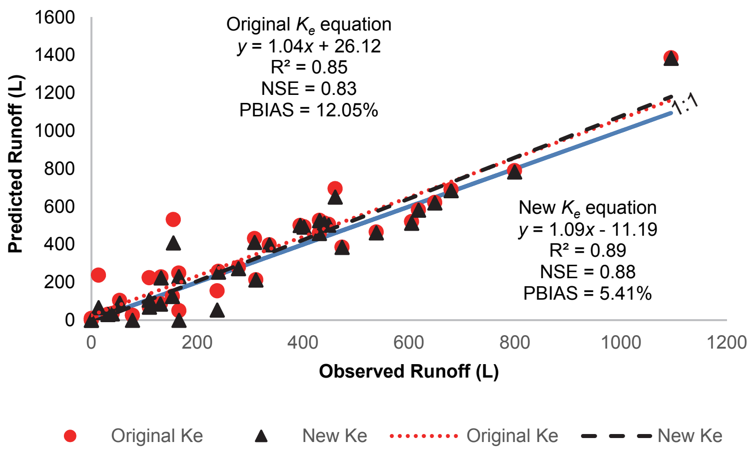

Figure 6. Observed versus predicted runoff for the 36 validation data points using the current and the newly developed estimation equations for the hydraulic conductivity (K_e).

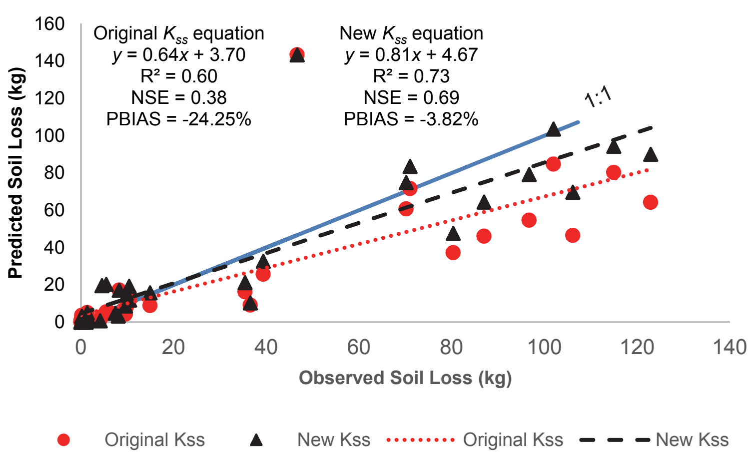

Figure 7. Observed versus predicted soil loss for the 36 validation data points using the current and the newly developed estimation equations for sheet and splash erodibility (K_{ss}).

ating K_{ss} on the calibration data, while estimates of K_e from equation 9 were used for the validation data. The percent bias of the additive K_{ss} model was maintained within the same order of magnitude across the calibration and validation data (PBIAS = 4.25% for the calibration data and -3.82% for the validation data).

Effect of Sodicity on Performance

Figure 8 compares the performance of the original and newly developed K_e estimation equations in predicting runoff volumes when the experimental data were divided into non-sodic (SAR ≤ 15, fig. 8a) and sodic (SAR > 15, fig. 8b) soils. Overall, equation 2 performed similarly for sodic and non-sodic soils but with a stronger positive bias for non-sodic soils. NSE values were similar at 0.69 and 0.70 for non-sodic and sodic soils, respectively, as were R^2 values (0.77 and 0.78, respectively). However, PBIAS values were much higher for non-sodic soils (40.87%) compared to sodic soils (11.82%). The use of the saline K_e equation (eq. 9) resulted in a dramatic improvement in runoff prediction performance for non-sodic soils, with NSE = 0.81, PBIAS = 5.50%, and R^2 = 0.82, whereas improvements for sodic soils were milder (NSE = 0.75, PBIAS = 6.43, and R^2 = 0.78). It is important to note that runoff from sodic soils was higher on average than runoff from non-sodic soils (403 L ±104 L vs. 198 L ±209 L), and this difference in hydrologic response may have contributed to the observed difference in performance of the K_e estimation equations across soil sodicity.

Compared to the original RHEM K_{ss} equation (eq. 3), using the K_{ss} values estimated by the SAR-adjusted equation markedly improved soil loss prediction for sodic soils. For these soils, the NSE, R^2, and PBIAS improved from 0.46, 0.77, and -24.37%, respectively, with equation 3 to 0.87, 0.89, and -5.32%, respectively, with the SAR-adjusted equation (fig. 9). However, for non-sodic soils, the improvements were marginal, with NSE, R^2, and PBIAS changing from 0.45, 0.55, and 38.49% to 0.46, 0.57, and 35.46%, respectively. This result suggests that the new K_{ss} equation provided improvements mostly on sodic sites but did not adversely impact soil loss prediction on non-sodic sites.

Salt Load Prediction

The relationship between soil loss and TDS is shown in figure 10. The linear model was adequate to predict runoff chemistry from its sediment concentration (R^2 = 0.94). TDS was related to SL through a positive relationship. Based on the equation of the linear model in figure 10, a 1 kg change in total soil loss resulted in a 2.36 g change in TDS (p = 0.00). In other words, the average salt to sediment mass ratio of the runoff was 2.36×10^{-3} g g^{-1}, or 0.24%. The non-zero

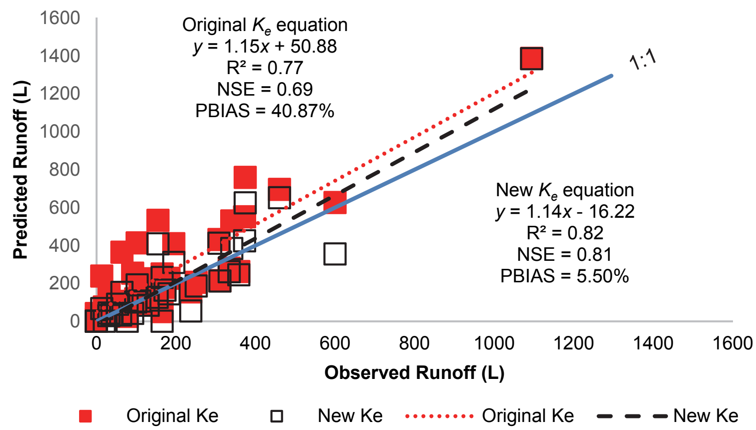

(a)

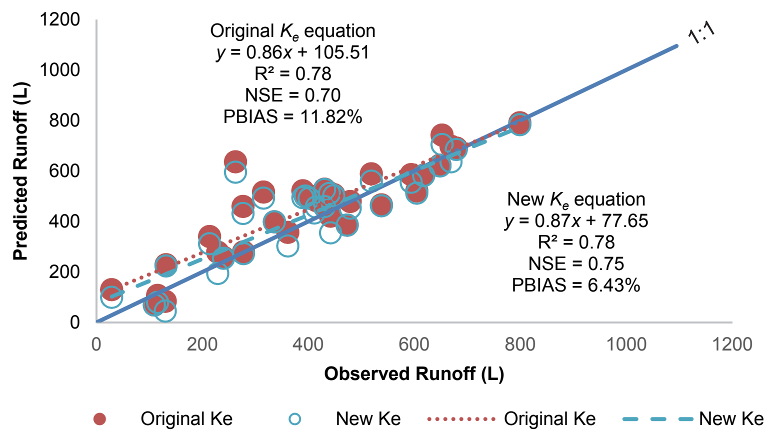

(b)

Figure 8. Observed versus predicted runoff for (a) non-sodic soils (*n* = 36) and (b) sodic soils (*n* = 36).

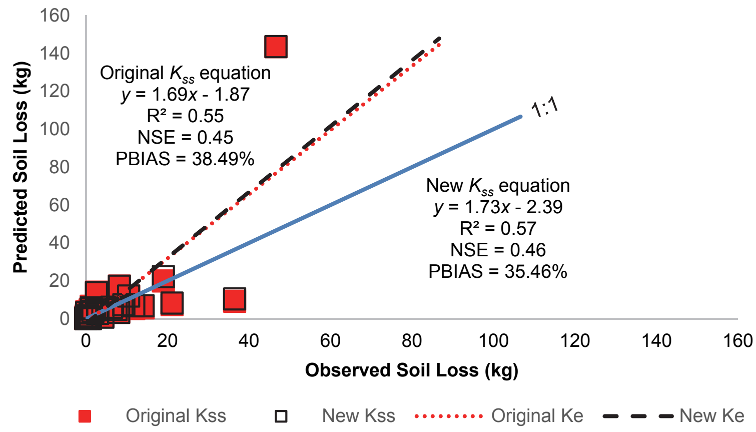

(a)

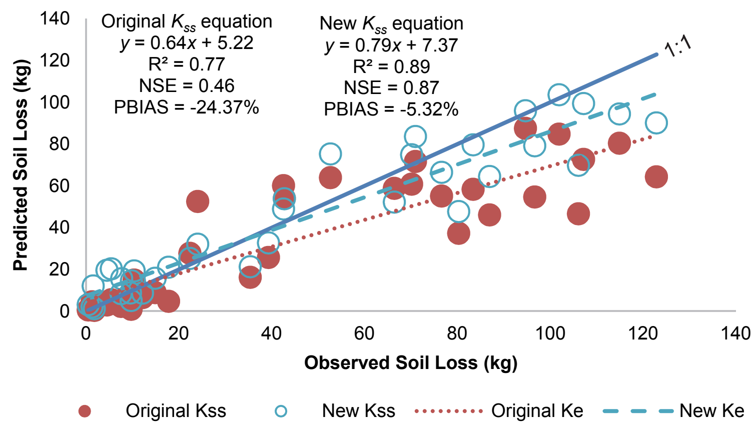

(b)

Figure 9. Observed versus predicted soil loss for (a) non-sodic soils and (b) sodic soils.

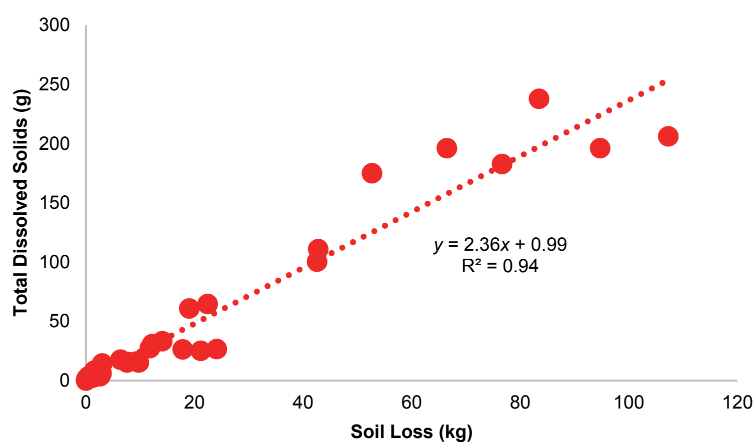

Figure 10. Relationship between cumulative soil loss and cumulative dissolved solids measured in runoff.

intercept of the linear model was not statistically significant. The equation used for predicting TDS from soil loss was therefore:

$$\mathrm{TDS} = 2.36 \times \mathrm{SL} + 0.99 \tag{10}$$

Figure 11 shows that equation 10 performed well in predicting TDS when RHEM-predicted SL values were used on the calibration data (fig. 11a) and the validation data (fig. 11b). The improvement in soil loss prediction with the use of the newly developed saline equations was reflected in the TDS predictions as well. For the calibration data, NSE and R^2 improved from 0.75 and 0.83, respectively, with the

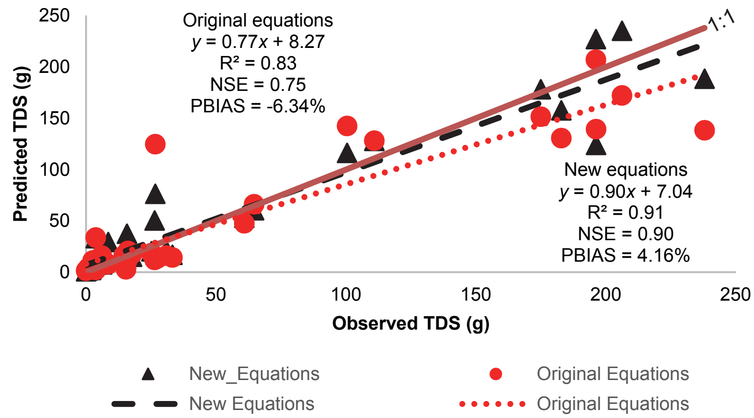

(a)

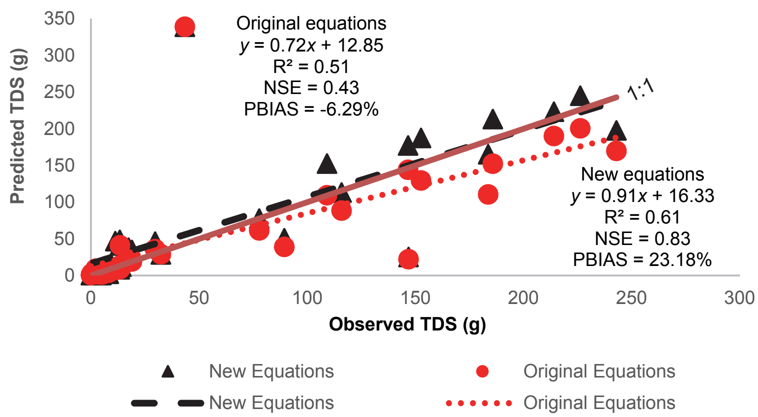

(b)

Figure 11. Observed versus predicted total dissolved solids (TDS) for (a) the 36 calibration data points and (b) the 36 validation using the current and newly developed estimation equations for K_e and K_{ss}.

original K_e and K_{ss} equations to 0.90 and 0.91, respectively, with the saline equations developed in this study. PBIAS was overall low but showed a mild improvement from -6.34% to 4.16%. For the validation data, a more dramatic improvement was noted for the NSE, which increased from 0.43 with the original K_e and K_{ss} equations to 0.83 with the saline equations. The R^2 value improved from 0.51 to 0.61, while PBIAS degraded from -6.29% to 23.18%. Soil loss predicted with the new K_e and K_{ss} equations underestimated the observed SL values, especially in the high SL range (fig. 7). These findings contrast with the overestimation of TDS shown in figure 11b when the new K_e and K_{ss} equations were used on the validation data, suggesting that this overprediction might be the result of the inherent variability in the runoff chemistry data.

Sensitivity Analysis

Figures 12 and 13 show the results of the sensitivity analysis performed on the newly developed K_e and K_{ss} models. Changes in parameter b' ($b' = 1.55b$) in equation 9 were inversely related to average changes in runoff amounts. Increases in b' are associated with an increase in hydraulic conductivity and thus an increase in total infiltration. As illustrated by the slope of the linear regression in figure 12, a 1% change in b' resulted in a 0.3% change in runoff volume. These values suggest a marginal effect of uncertainty in b' on the overall performance of equation 9 in predicting runoff, in contrast with the substantial improvement in performance (NSE increased by 30% and 6%, and |PBIAS| improved by 25.10 and 6.64 points for the calibration and validation data, respectively), when this new equation was used rather than equation 2 to predict K_e. The non-linear shape of the upper and lower 95% confidence bounds suggests that the sensitivity to b' is also a function of ground cover (plots with low ground cover are less affected by perturbations in b' than plots with high ground cover).

Changes to the SAR coefficient in the additive K_{ss} correction model (eq. 4) were also linearly related to average changes in total soil loss. In the case of soil loss, a low soil loss sensitivity to perturbations in the SAR coefficient was noted. A 1% change in the SAR coefficient yielded a 0.24% change in total runoff, in contrast with the notable improvements in prediction performance observed when K_{ss} estimations included the SAR term (NSE increased by 16% and 82%, and |PBIAS| improved by 2.22 and 20.43 points for the calibration and validation data, respectively). As in the case

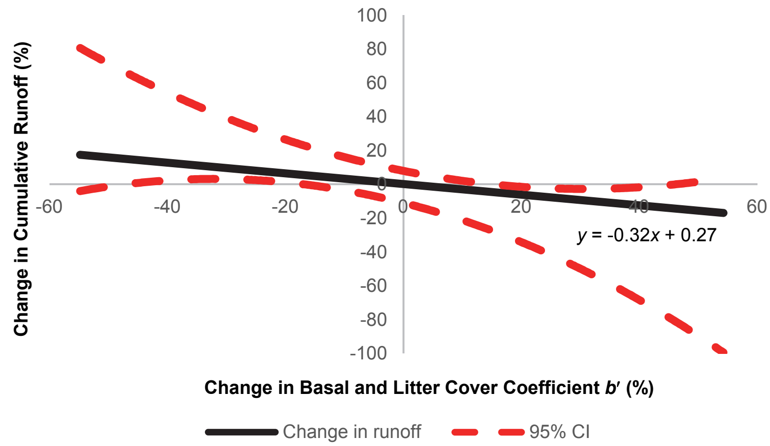

Figure 12. Average percent change in cumulative runoff volume as a function of disturbance in the calibrated b' for basal and litter cover in the hydraulic conductivity estimation equation. The average value of b' was 1.55, and basal and litter covers ranged from 0% to 78% and from 0% to 97%, respectively.

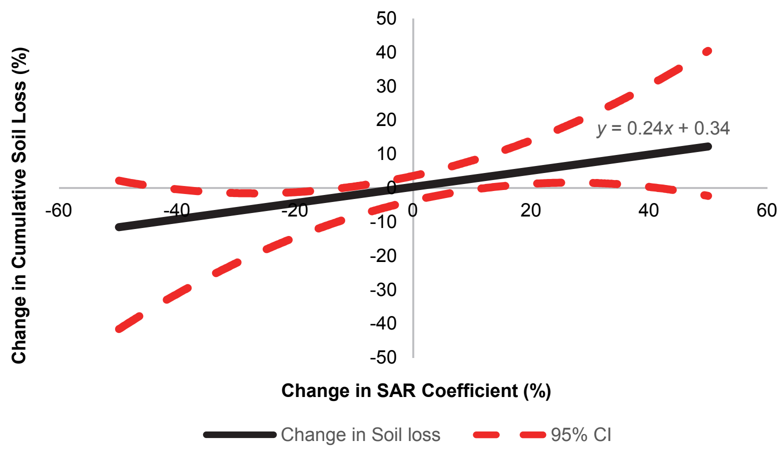

Figure 13. Average percent change in soil loss prediction as a function of changes in the sodium adsorption ratio (SAR) coefficient in sheet and splash erodibility (K_{ss}) prediction. The average value of the SAR coefficient was 642.4, and SAR values ranged from 0.07 to 56.4.

of K_e, the upper and lower 95% confidence bounds are nonlinear and suggest a sensitivity function that varies with soil SAR.

Discussion

Infiltration Rate on Saline Sites

In this study, we found that hydraulic conductivity values for saline sites were higher than those predicted by the current RHEM equations. A combination of factors could explain the higher infiltration rates observed on the saline sites compared to those predicted by RHEM. RHEM was developed from rainfall experiments conducted with a rotating boom simulator (e.g., Nearing et al., 2011; Simanton et al., 1991), while the experiments conducted in this study used the Walnut Gulch Rainfall Simulator (Paige et al., 2004). Potential variations in simulated raindrop size and kinetic energy between these two types of simulators could cause variations in infiltration response. At the same rainfall intensity, a more energetic event (larger droplet sizes) could result in rapid development of surface seal and a decrease in infiltration rate (e.g., Abrol et al., 2016; Romkens et al., 1990; Shainberg et al., 2003). Nevertheless, no data exist in the literature that compare simulated rainfall energy profiles between these two simulators. Another possible reason for a higher infiltration rate on the saline sites pertains to the physio-chemical effects of solute concentration on aggregate stability (Levy et al., 2003). The effects of solute concentration on soil hydraulic properties depend on the ions present in the solution and the soil (especially clay) mineralogy (Levy et al., 2003; She et al., 2015). Overall, an increase in solute concentration (excluding sodium) is associated with the development of strong water-stable aggregates and increased macroporosity, which in turn facilitate water movement through the soil profile (e.g., Agassi et al., 1994; Levy et al., 2003). Conversely, an increase in the proportion of sodium ions in the electrolyte mix exacerbates aggregate slaking, with potentially adverse effects on infiltration rate (Levy et al., 2003; She et al., 2015).

We found that runoff prediction was improved by equation 9 compared to equation 2 for both sodic and non-sodic soils, suggesting that the amplified K_e estimation in equa-

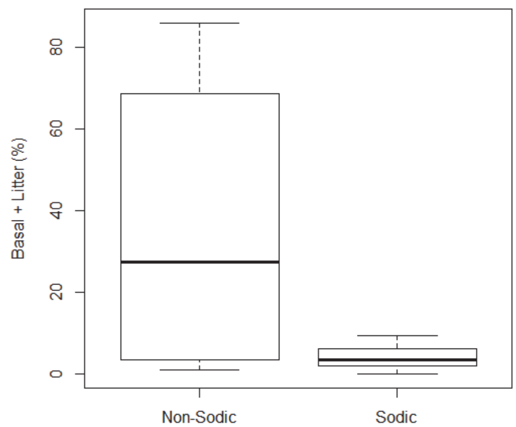

Figure 14. Distribution of the sum of basal and litter cover at sodic and non-sodic experimental sites.

tion 9 also applied to sites where sodium content was high. Nevertheless, litter and basal cover was lower on average at sodic sites than at non-sodic sites (fig. 14), which may have limited potentially adverse influences of the coefficient $b' = 1.55b$ in equation 9 on K_e estimation for sodic sites.

Soil Erosion and Sodicity

Soil erosion prediction was greatly improved by the inclusion of SAR in the sheet and splash erodibility estimation equation. In our study, soils high in sodium content (SAR > 15) benefited the most from the K_{ss} adjustment for SAR. Sodic soils are susceptible to clay swelling and dispersion when the total aqueous electrolyte concentration is below a critical flocculation concentration threshold (Sumner, 1993). An increase in dispersion not only increases runoff volumes through lowering of hydraulic conductivity and crust formation but also results in increased aggregate slaking, detachment by raindrop impact, and transport in runoff (Levy et al., 2003; Sumner, 1993; Tang et al., 2006). Simanton et al. (1991) described a rainfall simulation site in salt desert shrubs with a highly erodible soil surface marked by visible rills and measured excessive erosion rates compared to experimental sites in other rangeland communities. Soil at this highly erodible experimental site was mapped as Degater soil series (fine, smectitic, mesic Ustic Haplocambids) with a silty clay texture and mapped SAR values ranging from 3 at the surface to 20 at 0.60 m depth. The mapped SAR values for this site are similar to some of the sites classified as sodic in the current study, which likely explains the excessive erosion rates measured by Simanton et al. (1991). When a conservative SAR value of 10 is assumed for this site (which is lower than the SAR > 15 used elsewhere in this study), predicted soil loss estimates for two plots at the Simanton et al. (1991) site under very wet initial conditions were 7.16 and 4.95 kg with the SAR-adjusted K_{ss} equation and 3.32 and 2.46 kg with the original K_{ss} equation (eq. 3). The SAR-adjusted soil loss prediction was closest to the observed soil loss values of 10.55 and 3.38 kg.

Salt Load Prediction in Runoff

Early efforts to predict salt load in runoff have identified a close association between dissolved solids and transported sediments (Evangelou, 1981; Laronne and Shen, 1982; Ponce et al., 1975). Laronne and Shen (1982) mentioned the possibility of developing a predictive tool based on the regression between runoff solute content and sediment concentration. These early observations are consistent with the strong linear relationship between cumulative soil loss and TDS found in this study. Salts are picked up in runoff by the same mechanisms that detach and transport sediments, making sediment a strong predictor of runoff salt load. The initial attempt by Laronne and Shen (1982) to relate runoff salinity to runoff flow unit power (a function of discharge and slope) was improved and generalized with the use of the process-based model RHEM, which successfully captured the effects of various soil biophysical factors and topography on the susceptibility of modeled hillslopes to produce sediments, runoff, and salts. This model can now be used by land and resource managers as an effective tool to assess the salt load potential from saline hillslopes.

Conclusions

Parameter estimation equations have been developed to predict soil effective hydraulic conductivity (K_e) and sheet and splash erodibility (K_{ss}) on saline and sodic rangelands. Effective hydraulic conductivity on these sites was underestimated by the current RHEM K_e estimation, which required a magnified ground cover effect in the K_e estimation equation to accurately predict runoff on saline rangelands. The NSE, R^2, and PBIAS values for runoff improved from 0.56, 0.68, and 32.03%, respectively, to 0.73, 0.74, and 6.93% for the 36 calibration data points when the current K_e estimation equation was replaced with the updated K_e equation. The improved performance of the newly developed K_e estimation equation over the current K_e equation was maintained for the 36 validation data points used in this study. For these validation points, NSE and R^2 were mildly improved (0.83 and 0.85 vs. 0.88 and 0.89), while PBIAS showed a more substantial improvement from 12.05% to 5.41%. Soil loss prediction was significantly affected by soil SAR.

The current K_{ss} estimation equation used in RHEM was inadequate at predicting soil loss, especially on sodic sites (SAR > 15). Across all calibration data (sodic and non-sodic), the original K_{ss} equation yielded NSE, R^2, and PBIAS on soil loss prediction of 0.81, 0.85, and -6.47%, respectively, while the SAR-adjusted K_{ss} equation developed in this study yielded values of 0.94, 0.94, and 4.25% for these performance measures. Performance on the validation data improved from NSE = 0.38, R^2 = 0.60, and PBIAS = -24.25% to NSE = 0.69, R^2 = 0.73, and PBIAS = -3.82% when the original K_{ss} estimation equation was replaced with the SAR-adjusted equation developed in this study. Performance improvement with the integration of SAR into the K_{ss} estimation was dramatic on sodic soils but marginal on non-sodic soils. Conversely, the newly developed K_e estimation equation resulted in substantial runoff prediction improvements on non-sodic soils, while sodic soils experienced only mild improvements. Salt load was related to soil loss through a strong linear model (R^2 = 0.94), which performed well in estimating runoff salt load from RHEM-predicted soil loss

(NSE = 0.90, R^2 = 0.91, and PBIAS = 4.16% for the calibration data and NSE = 0.83, R^2 = 0.61, and PBIAS = 23.18% for the validation data). Sensitivity analyses on the K_e and K_{ss} equations developed in this study revealed low sensitivity of runoff and soil prediction to input parameter prediction, in contrast with the sizable improvement in prediction performance due to these newly developed equations.

ACKNOWLEDGEMENTS

This study was conducted as a collaborative effort between the Bureau of Reclamation, the Bureau of Land Management, the USDA Agricultural Research Service, and the University of Nevada, Reno. Initial funding was provided by the Bureau of Land Management (Agreement No. LI4PG00252) and the Bureau of Reclamation (Agreement No. R15PG00123).

REFERENCES

Abrol, V., Ben-Hur, M., Verheijen, F. G., Keizer, J. J., Martins, M. A., Tenaw, H., ... Graber, E. R. (2016). Biochar effects on soil water infiltration and erosion under seal formation conditions: Rainfall simulation experiment. *J. Soils Sediments, 16*(12), 2709-2719. https://doi.org/10.1007/s11368-016-1448-8

Agassi, M., Shainberg, I., & Vandermerwe, D. (1994). Effect of water salinity on inter-rill erosion and infiltration: Laboratory study. *Australian J. Soil Res., 32*(3), 595-601. https://doi.org/10.1071/sr9940595

Al-Hamdan, O. Z., Hernandez, M., Pierson, F. B., Nearing, M. A., Williams, C. J., Stone, J. J., ... Weltz, M. A. (2015). Rangeland Hydrology and Erosion Model (RHEM) enhancements for applications on disturbed rangelands. *Hydrol. Proc., 29*(3), 445-457. https://doi.org/10.1002/hyp.10167

Belnap, J., Wilcox, B. P., Van Scoyoc, M. W., & Phillips, S. L. (2013). Successional stage of biological soil crusts: An accurate indicator of ecohydrological condition. *Ecohydrology, 6*(3), 474-482. https://doi.org/10.1002/eco.1281

Blackburn, W. H. (1980). Universal soil loss equation and rangelands. *Proc. Symposium on Watershed Management* (pp. 164-175). Reston, VA: ASCE.

Blackman, W. C., Rouse, J. V., Schillinger, G. R., & Shafer, W. H. (1973). Mineral pollution in the Colorado River basin. *J. Water Pollut. Control Fed., 45*(7), 1517-1557. Retrieved from http://www.jstor.org/stable/25037925

Bundy, L. G., & Meisinger, J. J. (1994). Nitrogen availability indices. In R. W. Weaver (Ed.), *Methods of soil analysis, Part 2* (Vol. 5, pp. 951-984). Madison, WI: ASA, SSSA.

Bureau of Reclamation. (2005). Quality of water: Colorado River basin. Progress Report No. 22. Washington, DC: U.S. Bureau of Reclamation. Retrieved from http://www.usbr.gov/uc/progact/salinity/pdfs/PR22.pdf

Cadaret, E. M., McGwire, K. C., Nouwakpo, S. K., Weltz, M. A., & Saito, L. (2016a). Vegetation canopy cover effects on sediment erosion processes in the upper Colorado River basin Mancos Shale formation, Price, Utah, USA. *Catena, 147*, 334-344. http://dx.doi.org/10.1016/j.catena.2016.06.043

Cadaret, E. M., Nouwakpo, S. K., McGwire, K. C., Weltz, M. A., & Blank, R. R. (2016b). Experimental investigation of the effect of vegetation on soil, sediment erosion, and salt transport processes in the upper Colorado River basin Mancos Shale formation, Price, Utah, USA. *Catena, 147*, 650-662. http://dx.doi.org/10.1016/j.catena.2016.08.024

Evangelou, V. P. (1981). Chemical and mineralogical composition and behavior of the Mancos Shale as a diffuse source of salts in the upper Colorado River basin. PhD diss. Davis, CA: University of California.

Flanagan, D. C., & Nearing, M. A. (1995). USDA Water Erosion Prediction Project: Hillslope profile and watershed model documentation. NSERL Report No. 10. West Lafayette, IN: USDA-ARS National Soil Erosion Research Laboratory.

Foster, G. R., Simanton, J. R., Renard, K. G., Lane, L. J., & Osborn, H. B. (1981). Application of the Universal Soil Loss Equation to rangelands on a per-storm basis: Discussion. *J. Range Mgmt., 34*(2), 161-165. https://doi.org/10.2307/3898140

Hart, G. E. (1984). Erosion from simulated rainfall on mountain rangeland in Utah. *J. Soil Water Cons., 39*(5), 330-334.

Hernandez, M., Nearing, M. A., Al-Hamdan, O. Z., Pierson, F. B., Armendariz, G., Weltz, M. A., ... Holifield Collins, C. D. (2017). The Rangeland Hydrology and Erosion Model: A dynamic approach for predicting soil loss on rangelands. *Water Resour. Res., 53*(11), 9368-9391. https://doi.org/10.1002/2017WR020651

Hernandez, M., Nearing, M. A., Stone, J. J., Pierson, F. B., Wei, H., Spaeth, K. E., ... Goodrich, D. C. (2013). Application of a rangeland soil erosion model using National Resources Inventory data in southeastern Arizona. *J. Soil Water Cons., 68*(6), 512-525. https://doi.org/10.2489/jswc.68.6.512

Houska, T., Kraft, P., Chamorro-Chavez, A., & Breuer, L. (2015). SPOTting model parameters using a ready-made Python package. *PLoS One, 10*(12). https://doi.org/10.1371/journal.pone.0145180

Kenney, T. A., Gerner, S. J., Buto, S. G., & Spangler, L. E. (2009). Spatially referenced statistical assessment of dissolved-solids load sources and transport in streams of the upper Colorado River basin. USGS Scientific Investigations Report. Reston, VA: U.S.Geological Survey. Retrieved from http://pubs.usgs.gov/sir/2009/5007

Laronne, J. B., & Shen, H. W. (1982). The effect of erosion on solute pickup from Mancos Shale hillslopes, Colorado, USA. *J. Hydrol., 59*(1-2), 189-207. https://doi.org/10.1016/0022-1694(82)90011-7

Levy, G. J., Mamedov, A. I., & Goldstein, D. (2003). Sodicity and water quality effects on slaking of aggregates from semi-arid soils. *Soil Sci., 168*(8), 552-562. https://doi.org/10.1097/01.ss.0000085050.25696.52

Lisenbee, W. A., Fox, G. A., Saenz, A., & Miller, R. B. (2017). Comparison of field jet erosion tests and WEPP-predicted erodibility parameters for varying land cover. *Trans. ASABE, 60*(1), 173-184. https://doi.org/10.13031/trans.12012

Mubarak, A., & Olsen, R. A. (1976). Immiscible displacement of soil solution by centrifugation. *SSSA J., 40*(2), 329-331.

Nearing, M. A., Wei, H., Stone, J. J., Pierson, F. B., Spaeth, K. E., Weltz, M. A., ... Hernandez, M. (2011). A rangeland hydrology and erosion model. *Trans. ASABE, 54*(3), 901-908. https://doi.org/10.13031/2013.37115

Nouwakpo, S. K., Weltz, M., Hernandez, M., Champa, T., & Fisher, J. (2016). Performance of the Rangeland Hydrology and Erosion Model for runoff and erosion assessment on a semiarid reclaimed construction site. *J. Soil Water Cons., 71*(3), 220-236. https://doi.org/10.2489/jswc.71.3.220

NRCS. (2006). Land resource regions and major land resource areas of the United States, the Caribbean, and the Pacific basin. USDA Handbook 296. Washington, DC: USDA Natural Resources Conservation Service.

Paige, G. B., Stone, J. J., Smith, J. R., & Kennedy, J. R. (2004). The Walnut Gulch Rainfall Simulator: A computer-controlled variable intensity rainfall simulator. *Appl. Eng. Agric., 20*(1), 25-31. https://doi.org/10.13031/2013.15691

Ponce, S. L., Hawkins, R. H., Jurinak, J. J., Gifford, G. F., & Riley, J. R. (1975). Surface runoff and its effect on diffuse salt production from Mancos Shale members. *Proc. Symp. on Watershed Management* (pp. 140-168). Reston, VA: U.S.Geological Survey. Retrieved from http://cedb.asce.org/cgi/WWWdisplay.cgi?24065

R Development Core Team. (2015). R: A language and environment for statistical computing. Vienna, Austria: R Foundation for Statistical Computing. Retrieved from http://www.r-project.org/

Romkens, M. J. M., Prasad, S. N., & Whisle, F. D. (1990). Surface sealing and infiltration. In M. G. Anderson, & I. P. Burt (Eds.), *Process studies in hillslope hydrology* (pp. 127-172). Hoboken, NJ: John Wiley & Sons.

Shainberg, I., Mamedov, A. I., & Levy, G. J. (2003). Role of wetting rate and rain energy in seal formation and erosion. *Soil Sci., 168*(1), 54-62. https://doi.org/10.1097/00010694-200301000-00007

She, D. L., Gao, X. M., Wang, P., Xu, W. T., Liu, Y. Y., & Liu, Y. (2015). Comparison of soil hydraulic properties with different levels of soil salinity and sodicity. *Arabian J. Geosci., 8*(8), 5351-5360. https://doi.org/10.1007/s12517-014-1514-8

Simanton, J. R., Weltz, M. A., & Larsen, H. D. (1991). Rangeland experiments to parameterize the Water Erosion Prediction Project model: Vegetation canopy cover effects. *J. Range Mgmt., 44*(3), 276-282. https://doi.org/10.2307/4002957

Spaeth, K. E., Pierson, F. B., Weltz, M. A., & Blackburn, W. H. (2003). Evaluation of USLE and RUSLE estimated soil loss on rangeland. *J. Range Mgmt., 56*(3), 234-246. https://doi.org/10.2307/4003812

Sumner, M. E. (1993). Sodic soils: New perspectives. *Australian J. Soil Res., 31*(6), 683-750. https://doi.org/10.1071/sr9930683

Tang, Z., Lei, T., Yu, J., Shainberg, I., Mamedov, A. I., Ben-Hur, M., & Levy, G. J. (2006). Runoff and interrill erosion in sodic soils treated with dry PAM and phosphogypsum. *SSSA J., 70*(2), 679-690. https://doi.org/10.2136/sssaj2004.0395

Weltz, M. A., Jolley, L., Hernandez, M., E. Spaeth, K., Rossi, C., Talbot, C., ... Morris, C. (2014). Estimating conservation needs for rangelands using USDA national resources inventory assessments. *Trans. ASABE, 57*(6), 1559-1570. https://doi.org/10.13031/trans.57.10030

Weltz, M. A., Kidwell, M. R., & Fox, H. D. (1998). Invited synthesis paper: Influence of abiotic and biotic factors in measuring and modeling soil erosion on rangelands: State of knowledge. *J. Range Mgmt., 51*(5), 482-495. https://doi.org/10.2307/4003363

Williams, C. J., Pierson, F. B., Spaeth, K. E., Brown, J. R., Al-Hamdan, O. Z., Weltz, M. A., ... Nichols, M. H. (2016). Incorporating hydrologic data and ecohydrologic relationships into ecological site descriptions. *Rangeland Ecol. Mgmt., 69*(1), 4-19. http://dx.doi.org/10.1016/j.rama.2015.10.001

Zhang, Y., Hernandez, M., Anson, E., Nearing, M. A., Wei, H., Stone, J. J., & Heilman, R. (2012). Modeling climate change effects on runoff and soil erosion in southeastern Arizona rangelands and implications for mitigation with conservation practices. *J. Soil Water Cons., 67*(5), 390-405. https://doi.org/10.2489/jswc.67.5.390